CETRA2022 11-13 May 2022, Pula, Croatia
7th International Conferenceon Road and Rail Infrastructure

3-DIMENSIONAL BEARING CAPACITY ENVELOPES OF BRIDGE SHALLOW FOUNDATIONS ON COHESIONLESS SOILS AND SCOUR EFFECTS

Konstantina Papadopoulou
National Technical University of Athens, Greece

Abstract

The effects of the combined loading on the bearing capacity (B.C.) shallow bridge foundations on cohesionless soil are investigated by 2D and 3D finite element analyses (F.E.A.), in conjunction with the main parameters involved, as the embedment depth. For the better visual understanding how the various loading or inherent parameters affect the ultimate B.C. the results of F.E.A. are presented as interaction diagrams of the normalized vertical load, moment and horizontal load. The scour effects on the B.C. of shallow foundation are investigated, through the normalized scour depth.

Keywords: shallow foundations, cohesionless soil, embedment depth, scour, F.E. analyses

1 Introduction

Spread footings continue to be an attractive type of bridge foundations, due to the simplicity of construction and the low cost. On the other hand, piers and abutments of many old bridges over the world were supported on shallow foundations and it is often necessary to have a sense of their vulnerability, mainly during flood events. The settlements of shallow bridge foundations on cohesionless soils in most cases are not significant, while systematic observations and evaluation of data indicated that considerably higher displacements are tolerable than those adopted at the past i.e.[1]. Consequently, the Ultimate Limit States criteria have a decisively influence on the design and the vulnerability of bridge foundations in many cases.

Scour is a major reason for bridge foundation failure. Case histories of bridge failures due to scour were analyzed and discussed [2]. The hydraulic performance of shallow bridge foundations was extensively investigated (i.e. Federal Highway Administration, [3]), but the procedures aiming at the estimation of the vulnerability of theses, in many cases overlook the geotechnical factors.

In the present paper the following issues are examined, based on 2D and 3D F.E.: i) The embedment depth effect on the bearing capacity of shallow foundations on cohesionless soils for the general case of combined loading M, V, H. ii) The scour effects on the bearing capacity. The results are presented as interaction diagrams, from sections of the bearing strength surfaces (BSS) by representative planes.

DOI: https://doi.org/10.5592/CO/CETRA.2022.1407

2 Depth effects on the bearing capacity of footings on cohesionless soils

In case of cohesionless soil, assuming horizontal foundation base, the ultimate vertical load, for the combined loading V, M, H, according to EN 1997-1 [4], which is based on a former version of DIN 4017 [5], is given by the equation:

$$V_u = A' \cdot (q' \cdot \mathbf{N}_q \cdot s_q \cdot i_q + 0.5 \cdot \boldsymbol{\gamma}' \cdot \mathbf{B}' \cdot \mathbf{N}_\gamma \cdot s_\gamma \cdot \mathbf{i}_\gamma) \quad (1)$$

where $A' = \mathbf{B}'L'$ is the effective contact area, $\mathbf{B}'$, L' the effective width and length of footings, q' the effective overburden pressure at the footing base, N_q, N_γ, the B.C. factors, s_q, s_γ the shape factors and i_q, i_γ the inclination correction coefficients.
Semi-empirical coefficients accounting the effects of shape, depth, eccentricity and inclination of loadings are available to be applied on the equations, i.e.[6]. Comparisons of various proposals for the shape and inclination were presented and discussed at the past (i.e.[7]). The same important factors were investigated using numerical approach by [8]. The effect of embedment depth D on the B.C. is of great importance and it is taken into account, according to Eq.(1) through the effective overburden pressure q' at the footing base.

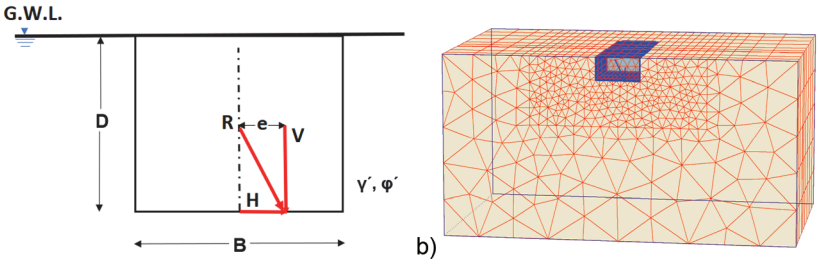

Figure 1 Rectangular footing on cohesionless soil: a) Combined loading V, M, H on rectangular footing, b) Example of 3D F.E. mesh

Following the conventional methods, a real problem according to Fig. 1a, could be simulated by a footing on the surface, which is loaded by a uniformly distributed load q'. This simplification is usual, even in FE analyses, as for example after [9]. In order to examine the effect of embedment depth, owing not only to the equivalent loading, $q' = \gamma' \cdot D$, FE analyses are carried out under 2D and 3D conditions, by the more realistic simulation as in Fig. 1b. In order to compare the FE results with those from the conventional method, firstly the simple case of vertical centric load at the base of a rectangular foundation is examined. The water table is considered at the surface, therefore $q' = \gamma' \cdot D$. The ultimate vertical load for a rectangular footing (L, B) corresponding to the conventional methods can be expressed at the normalized form:

$$\frac{V_u}{\gamma' \cdot L \cdot B^2} = \frac{D}{B} \cdot N_q \cdot S_q \frac{1}{2} N_\gamma \cdot S_\gamma \quad (2)$$

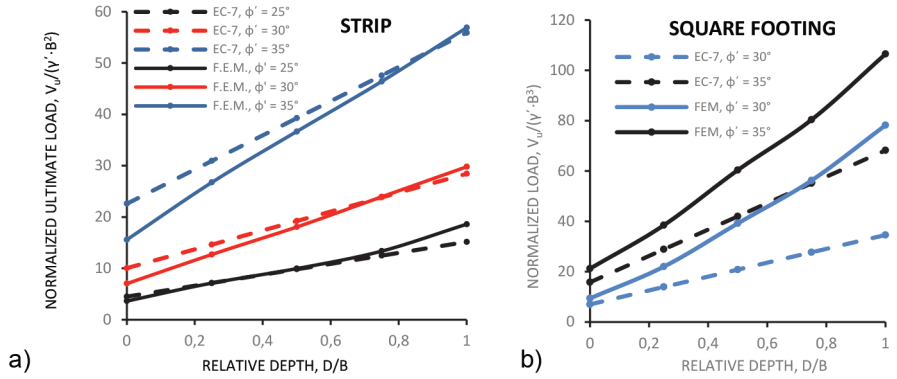

Figure 2 Effect of the foundation depth on the normalized ultimate load: cohesionless soils, vertical loads: a) Strip footing, b) Square

Following the Eq. (2) and the FEA results, comparative diagrams are presented in Figs. 2a and 2b, for strip and square footings, respectively, where the following can be observed:

- For strip footings and low ratios D/B, the normalized values of the ultimate loads, according to Eq. (2), are higher than those resulted from the FEA, due to the lower values of the B.C. factor N_γ in the latter case. On the contrary, for higher values D/B, the initial differences are decreased, owing to the higher rate of increase of V_u with increasing embedment depth from theFEA.
- For square footings, the normalized ultimate load values from FEA are quite higher, independently of the embedment depth. Therefore, the effect of D/B on the B.C. is considerably greater, in accordance with the FEA.

Evidently, the failure mechanism for the real case of foundation at depth D is different from the simplified simulation of depth by an equivalent loading q′ at the surface, as it is shown in Figs. 3a and 3b for a centric vertical load and an eccentric and highly inclined load respectively.

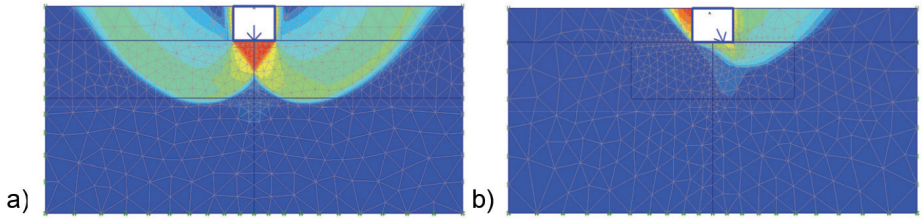

Figure 3 Failure mechanisms of embedded footing: a) centric vertical load, b) eccentric and inclined load

The simultaneous effects of the relative depth and the shape of footing on the normalized ultimate load are illustrated in Fig. 4, where the effect of embedment depth on the ultimate load V_u for rectangular footings, is considerably higher in finite element analysis method than this from Eqs. (1) and (2) and the relevant shape factors s_q and s_γ.

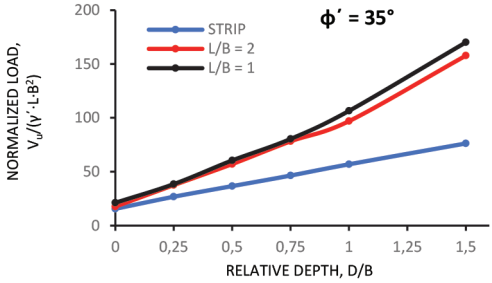

Figure 4 Effect of shape on the normalized ultimate load of embedded footing

3 Interaction diagrams for combined loadings

In the general case of loading V, M, H (vertical load, moment and shear force), all combinations, which lead to shear failure, form a three-dimensional bearing strength surface (B.S.S.) These surfaces were investigated by many authors, as for example by [10] and [11]. A convenient way to examine a B.S.S. is to use the normalized loading values, according to the relationships:

$$v = \frac{V}{V_{u,o}}; \quad m = \frac{M}{V_{u,o} \cdot B}; \quad h = \frac{H}{V_{u,o}} \tag{3}$$

where the basic normalized loading parameter, $V_{u,o}$ is the ultimate vertical and centric load. Comparative interaction diagrams resulting from the conventional B.C. methods and FEA are presented for the simplest case of strip footing on the surface. In Fig. 5a, the interaction diagrams v-h resulting from the section of B.S.S. by a vertical plane at m = 0, are almost identical, so the inclination factor i_γ in the conventional method is verified by the FEA. However, in Fig. 5b, presenting the interaction diagrams v-m for two cases, h = 0 and h = 0.06, it can be observed that despite the fact that the differences are not appreciable for vertical load, the simultaneous effect of eccentricity and inclination results in significantly lower values in conventional methods, for the inclined loading.

The effect of the inclination of loading through the normalized value h, for square footing and normalized embedment depth D/B = 0.5, on the interaction diagrams v-m is shown in Fig. 6a, while the diagram v-h (for m = 0) is presented in Fig. 6b. From Fig. 6b and FEA for greater ratios D/B, it can be concluded that the inclination of the loading, H/V = h/v increases with increasing embedment depth, therefore for centric and inclined load (m = 0) relatively high horizontal loads, H, can be undertaken, even for very low vertical ones, V. The effects of the embedment depth on the interaction diagrams in the simple case of strip footing are illustrated in Fig. 7a (v-m and h = 0) and 7b (v-h and m = 0). For increasing ratio D/B, the ability to undertake either higher horizontal loads or higher moments is evident.

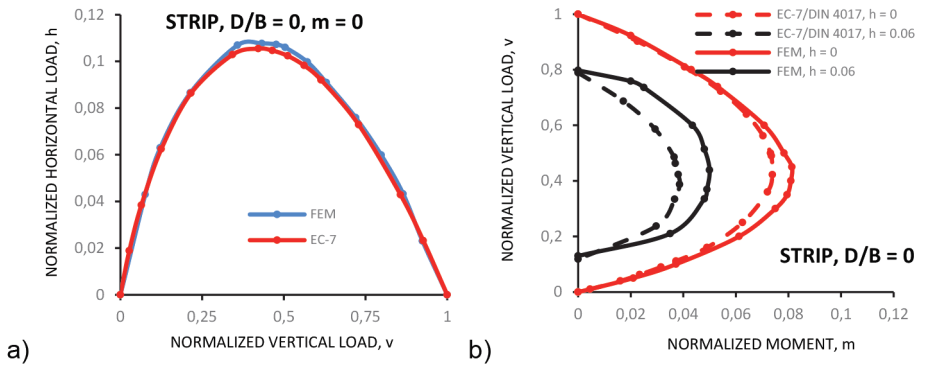

Figure 5 Strip on cohesionless soil. Comparative diagrams from FE analyses (solid lines) and after EC-7/DIN

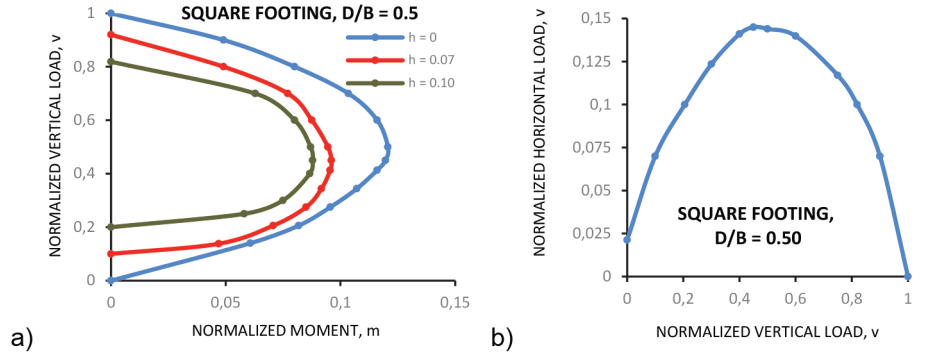

4017 (dashed lines): a) v-h on the plane m = 0, b) v-m (h = 0 and h = 0.06)

Figure 6 Square footing on cohesionless soil, D/B = 0.5: a) v-m sections for various h, b) v-h (m = 0 plane)

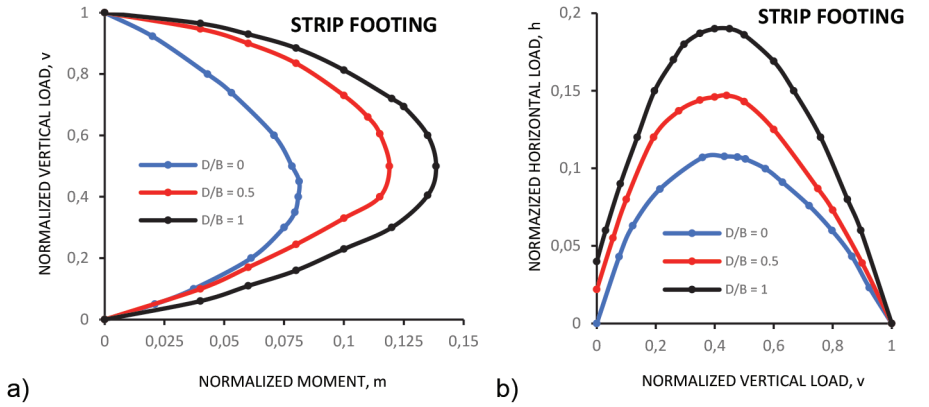

Figure 7 Strip on cohesionless soil: Effect of the embedment depth on the interaction diagrams: a) m-v, b) v-h and m = 0.

4 Scour effects on the bearing capacity of shallow foundations

The loss of foundation soil in riverbed due to water flowing is associated with distinct mechanisms, form which more important are the general erosion and the local scour. The latter one is generated by the rapid variation of intensity and distribution of the water velocity and generally represents the most significant scour process, since this can reach great depths. Federico et al [12] presented a simple method to estimate the vulnerability of bridge foundations owing to scour, applying the conventional B.C. equation. The ultimate vertical load $V_{u,s}$ mainly depends on the effective, remaining foundation depth $D' = D - D_s$, (where D_s the scour depth and D the initial one) and the geometry of the vertical section at the foundation position. The key Fig. 8a refers to the case of general scour, while Fig. 8b presents a simplified cross section, where B_s is the base of the mechanism ($B_s > B$).

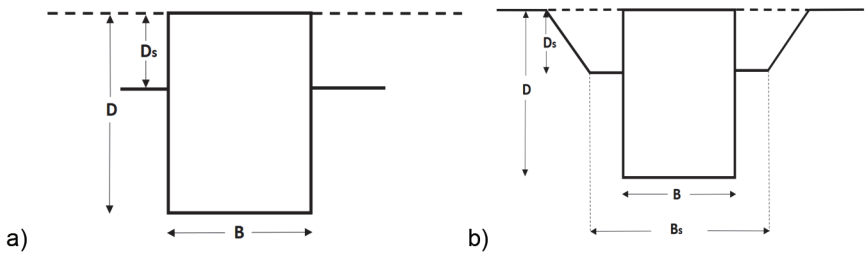

Figure 8 Key Figures: a) General erosion, b) Local scour

The differences of failure mode for the two scour cases, reflect on the ultimate vertical load, $V_{u,s}$. From relevant comparative FEA for strip footing, the effect of the relative scour depth D_s/D on the ratio $V_{u,s}/V_{u,o}$ is indicatively shown in Fig. 9, where $V_{u,o}$ is the ultimate load for the initial conditions, where $D_s = 0$ and $D' = D$. The decrease of the ultimate load with increasing scour ratio D_s/D is almost linear in case of general erosion and very significant. In Fig. 9, the ultimate load $V_{u,s}$ is approximately 20 % of the initial one for $D_s/D = 1$. On the contrary, in the case of local scour, the decrease of $V_{u,s}$ with increasing D_s/D is almost insignificant, if $D_s/D < 0.7$, even for the higher Bs/B ratios. The differences of the resulted values of the ultimate load $V_{u,s}$ for general and local scour and the same ratio D_s/D is explained by the failure mode in each case. The failure mechanism for local scour ($D_s/D = 0.75$) and eccentric inclined load is illustrated in Fig. 10.

In the case of local scour, representative interaction diagrams with $D_s/D = 0.75$ and $D/B = 1.50$ are shown in Fig. 11. The normalization value $V_{u,o}$ is the initial one, without scour, i.e. $D_s = 0$, thus the diagrams illustrate the relative decrease of all values v, m, h, due to the local scour. Despite the fact that the increase of the horizontal loading (through the normalized value h) results in a quite significant decrease of m values for any given value of vertical load, the ability to undertake combined loadings remains remarkable.

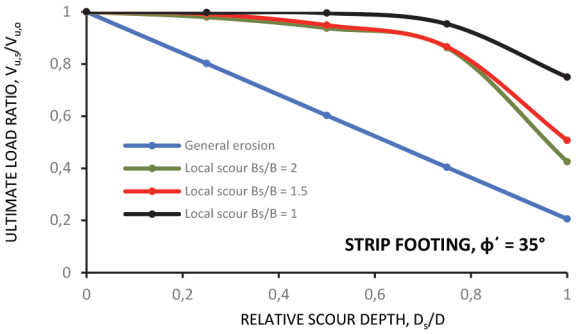

Figure 9 Effect of relative scour depth on the ultimate load ratio

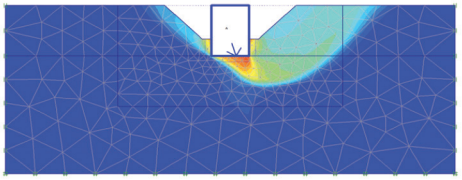

Figure 10 Local scour, D_s/D = 0, 75: Failure mechanism

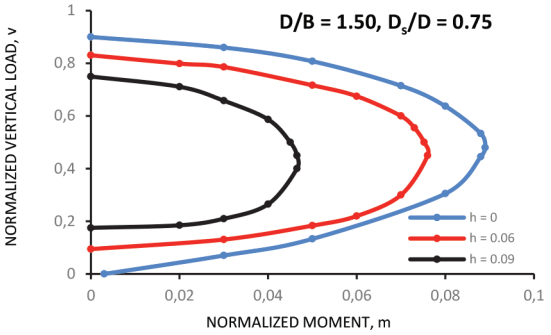

Figure 11 Local scour, D_s/D = 0.75: Effect of h on diagrams v-m

5 Conclusions

Following theFEA results, it can be concluded that the simultaneous effects of embedment depth, shape of the foundations, inclination and eccentricity of the loadings on the bearing capacity can not be approached by the product of coefficients e.t.c., according to the conventional methods, which it seems that considerably underestimate the ultimate loads in many cases. From the comparison of the interaction diagrams for increasing relative depth, it can be shown that the Bearing Strength surfaces become wider (at m direction) and higher (at h direction). Moreover, the BSS for given D/B surrounds the others corresponding to lower relative depths. The scour effects on the B.C. mainly depend on the type of scour (general erosion or local scour) and the scour depth, as well. Although the case of general erosion is the unfavourable one, for given D_s/D value, it may be noted that local scour, generally reaches greater depths.

Acknowledgements

This research is co-financed by Greece and the European Union (European Social Fund - ESF) through the Operational Programme «Human Resources Development, Education and Lifelong Learning» in the context of the project "Reinforcement of Postdoctoral Researchers - 2nd Cycle" (MIS-5033021), implemented by the State Scholarships Foundation (IKY).

References

[1] Paikowsky, S.: Serviceability in the design of bridge foundations, Conf. on Evaluation of Eurocode 7, pp.251-261, Trinity College, Dublin, 31 March - 1 April 2005.

[2] Lin, C., Han, J., Bennett, C., Persons, R.: Case history analysis of bridge failures due to scour. International Symposium of climate effects on Pavement and Infrastructure, University of Alaska, 2014.

[3] Federal Highway Administration: Hydraulic performance of shallow foundations for the support of vertical-wall bridge abutments. Publication N° FHWA-HRT-17-013, 2017.

[4] EN 1997-1: Geotechnical Design-Part 1: General rules, CEN, 2004.

[5] DIN 4017 Baugrund-Berechnung des Grundbruchwiderstands von Flachgründungen, 2006.

[6] Poulos, H.G., Carter J.P., Small, J.C.: Foundations and Retaining structures-research and practice. General Report, 15th International Conference on Soil Mechanics and Geotechnical Engineering, pp. 2533-2548, Istanbul, Turkey, 27-31 August 2001.

[7] Zadroga, B.: Bearing capacity of shallow foundations on non cohesive soils, Journal of Geotechnical Engineering, ASCE, 120 (1994) 11, pp.1991-2008

[8] Baars, S: The inclination and shape factors for the bearing capacity of footings. Soils and Foundations, 54 (2014) 5, pp. 985-993

[9] Krabbenhoft, S., Damkilde, L., Krabbenhoft, K.: Bearing capacity of strip footings in cohesionless soil subjected to eccentric and inclined loads, Int. J.Geomech., ASCE, 14 (2014) 3, 04014003

[10] Pender, M.: Bearing capacity surfaces implied in conventional capacity calculations, Géotechnique, 67 (2017) 4, pp. 313-324

[11] Vrettos, C., Seibel, E.: Bewertung von pseudo-statischen Methoden zum Grundbruchwiderstand von Fundamenten unter seismischer Beanspruchung, Bautechnik 95 (2018) 12, pp. 859-871

[12] Federico, F., Silvagni, G., Volpi, F.: Scour vulnerability of river bridge piers, Journal of Geotechnical and Geoenvironmental Eng., ASCE, 129 (2003) 10, pp. 890-899